

EXPERIMENTAL ANALYSIS OF THE EFFECT OF PLASMA ACTUATOR ON FLOW CONTROL ON NACA 4412 AIRFOIL

Gokcen Jurnal¹, Cem Kolbakir² and Ahmet Selim
Durna³
University of Samsun
Samsun, Turkey

Burak Karadag⁴
Surrey Space Centre, University of Surrey
Guildford, United Kingdom
University of Samsun, Samsun, Turkey

ABSTRACT

In this study, the effect of a DBD plasma actuator on controlling the flow over a 3D-printed NACA 4412 airfoil was experimentally examined. Firstly, plasma actuator installation was investigated on the flat plate for different dielectric layer thickness and electrode length. Secondly, smoke visualization experiments were performed with the printed airfoil for 8 different spanwise electrode configurations in a small-scale wind tunnel at a Reynolds number of 35000 to determine the optimum configuration. It was found that the plasma actuation effect is higher for the configurations that have multiple electrodes spread on the airfoil surface than the single electrode configurations. This effect reduces flow separation and delays the stall of the airfoil, which may be related to the boundary layer thickness, and the effect becomes more significant as the angle of attack decreases.

INTRODUCTION

Plasma, the fourth state of matter, have been studied for various applications in the aeronautics and astronautics industry, for example, icing mitigation [Kolbakir et al., 2019], ignition-combustion [Starikovskaia, 2006], space propulsion [Karadag et al., 2018], noise control [Al-Sadawi et al., 2019], and flow control [Greenblatt et al., 2008; Moreau, 2007; Neretti, 2016]. In recent years, plasma actuators have drawn considerable interest in the field of flow control. They have preferable features compared to passive flow control methods (e.g. slats on the leading edge, and slotted flaps on the trailing edge, vortex generators) and other active flow control methods (e.g. ultrasonic synthetic jet actuators), which have complicated mechanical design adding weight and volume to the overall system and act as a source of noise and vibration. Plasma actuators are light weight and easily mounted to the wings, and they do not include moving parts, respond fast, and work with lower energy compared to other active flow control devices [Cattafesta and Sheplak, 2011]. Therefore, researching the flow control effects of plasma actuators is important to provide their usage in future aerial vehicle designs.

¹ Undergraduate student in the Department of Aerospace Engineering, Email: gokcenjurnal[at]gmail.com

² Asst. Prof. in the Department of Aircraft Maintenance, Email: cem.kolbakir[at]samsun.edu.tr

³ Asst. Prof. in the Department of Aerospace Engineering, Email: ahmetselim.durna[at]samsun.edu.tr

⁴ Research Fellow in the Department of Electrical and Electronic Engineering at the University of Surrey and Asst. Prof. in the Department of Aerospace Engineering at the University of Samsun, Email: b.karadag[at]surrey.ac.uk

As it can be seen in Figure 1, Dielectric Barrier Discharge (DBD) plasma actuators used in aerodynamic flow control simply consists of the asymmetric positioning of two electrodes that have a dielectric layer in-between. The high voltage supplied to the electrodes generates a high electric field at the close proximity of the electrodes and ionizes the air. The created heavy ions are accelerated by the applied electric field and transfer momentum to the surrounding neutral gas by the ion-neutral collisions. In this way, a flow tangent to the surface is induced by the plasma actuator. The induced flow velocity can reach up to 8 m/s and plays an important role in the delay of flow separation at high angle of attack and the decrease of drag force. Sinusoidal voltages between the range of 5-50 kV and the frequencies of 1-100 kHz are generally used to ignite this type of plasma [Moreau, 2007].

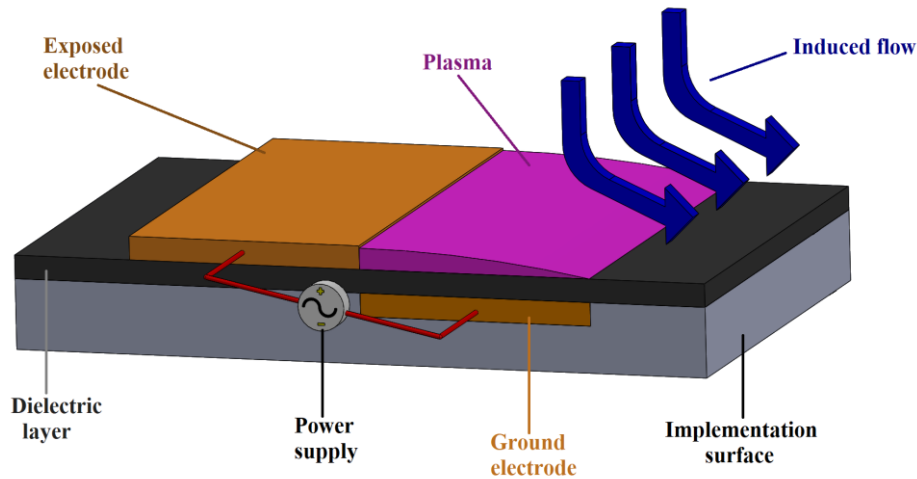


Figure 1: DBD plasma actuator diagram

The position of the DBD plasma actuators on the aerodynamic surfaces is a key point for the efficiency of the flow control efficiency. In order to ensure the optimum effect, the actuator has to be placed on the wing surface right before the flow detachment point [Neretti, 2016]. Greenblatt et al., in their experiments on a flat-plate airfoil and an Eppler E338 airfoil at the Reynolds number varied between 3000 and 50000, have observed that steady and pulsed control were provided thanks to the DBD plasma actuators applied on the leading edges of the aerodynamic bodies [Greenblatt et al., 2008]. Thomas et al. have studied the effects of parameters such as voltage, frequency, dielectric layer type and thickness, electrode geometry on the force induced by the DBD plasma actuator. It has been observed that the momentum transfer effect can increase up to a point with the usage of thinner dielectric layer and the increase of voltage and frequency; however, it has also been observed that this effect disappears when the plasma starts to be filamentary [Thomas et al., 2009]. Akansu et al. have observed that the flow detached from the leading edge reattaches by increasing the voltage provided to the plasma actuator [Akansu et al., 2013]. Little et al. have studied the flow detachments originated at the trailing edge and shown that the plasma actuator delays flow detachment and provide a decrease in drag force [Little et al., 2010]. Post et al. have shown in their experiments where Reynolds number varied between 77000 and 333000 that thanks to the plasma actuator the flow that detaches at high angles of attack from the leading edge, delays the stall by reattaching and the stall angle can be delayed up to 8° . In addition, an increase of up to 400% at the lift to drag ratio was also observed [Post and Corke, 2004].

In accordance with the data in the literature, it can be seen that the DBD plasma's momentum effect is satisfied at low Reynolds numbers. NACA 4412 airfoil has a high stall angle and it is suitable for use at low Reynolds numbers: however, plasma actuation hasn't been comprehensively studied in the literature. Previously Karadag et al. investigated the effects of a DBD plasma actuator qualitatively on aerodynamic characteristics of a 3D-printed NACA 4412 airfoil model and demonstrated that spanwise-generated electric wind is more effective

in the reattachment of the airflow over streamwise-generated one at a low Reynolds number [Karadag et al., 2021]. In this study, the effect of singular, dual and multiple spanwise plasma actuator configurations on various locations of the airfoil on flow control was investigated at a wider range of angles of attack. This work is mainly aimed at the research of the flow control effect of DBD plasma actuators on NACA 4412 airfoil. Observation of the most suitable, electrode configuration and plasma actuation parameters, such as dielectric layer thickness, electrical current parameters for plasma actuation and determination of the aerodynamic efficiency of different actuator configurations are the other points analyzed in this study.

METHOD

The research consists of two different parts: plasma formation on the flat plate, smoke flow visualization. Methods used for these parts were explained comprehensively in the following.

Plasma Actuators on the Flat Plate

Firstly, the installation of plasma actuators with different parameters such as dielectric layer thickness, electrode length, electrical voltage and frequency on a flat plate was investigated. Experiments were conducted in-still air to ensure stable and uniform plasma formation. The parameters obtained here were used in the installation of the plasma actuators on the airfoil in the flow visualization experiments. The parameters of the experiments which has made by changing the power supplies, electrode lengths and dielectric layer thickness are given in Table 1. The table can be interpreted as follows: for No. 5, an actuator which has 3 cm electrode length and 0.36 mm dielectric layer thickness was activated by an ozone generator power supply with 15kV voltage and 3kHz frequency or for No. 18, an actuator which has 10 cm electrode length and 0.72 mm dielectric layer thickness was activated by a neon power supply with 10kV voltage and 31kHz frequency.

Flow Visualization

Secondly, smoke flow visualization experiments were performed with TecQuipment AF17, a small-scaled, and open-circuit vertical airflow bench located at the Aerodynamic Research Laboratory of the University of Samsun. The operating flow velocity of the tunnel is 0.8-35 m/s and the dimensions of the tunnel test section are 26 x 26 x 4 cm (width x length x depth). The airfoil model used for flow visualization was made of PLA (Polylactic Acid) material using a 3-D printing technique with a chord length of 10 cm and a span of 4 cm.

Figure 2 shows positions of the electrodes on the airfoil. Each plasma actuator configuration corresponds to a combination of the powered electrodes. For example, only the electrode A is powered in the 1st configuration, while the electrodes A and C are powered simultaneously in the 4th configuration. 8 different plasma actuator configurations were tested in total on the same airfoil. Figure 3 shows the plasma formation on the airfoil for the 8th plasma actuator configuration in which all the electrode strips (A+B+C+D+E) were powered.

In the experiments, the angle of attack (α) was kept in the range of $0^\circ - 25^\circ$, and altered with 5° increments for both the plasma off and on cases and the experiments were repeated for each plasma actuator configuration (experimental error margin is estimated $\pm 1^\circ$). Finally, image processing methods were applied to the test results for reducing the effect of experimental errors on the results. In addition, image processing helps for interpretation of the results reliably [Jurnal et al., 2021].

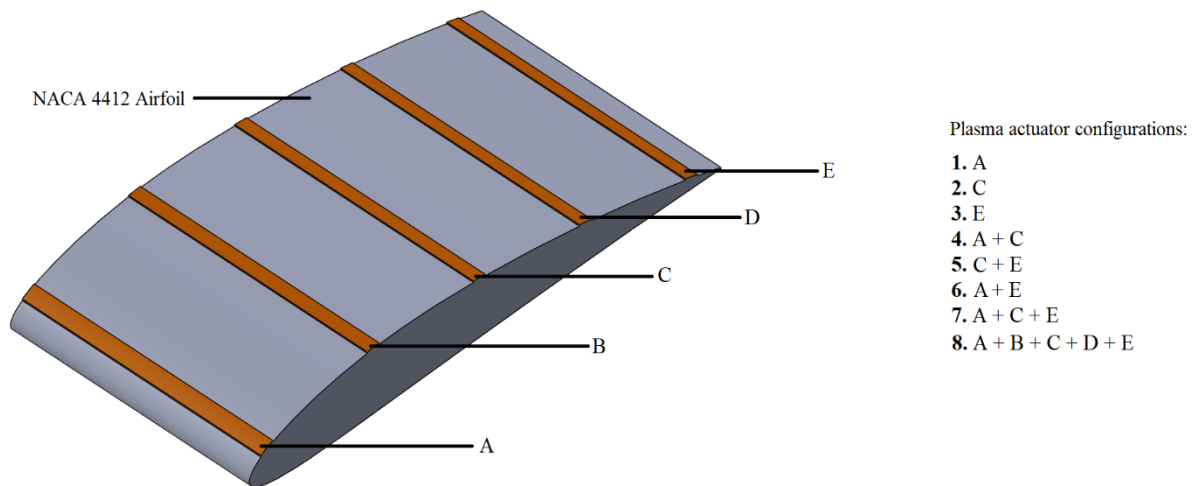


Figure 2: The positions of electrodes on the airfoil (only the exposed electrodes were shown)

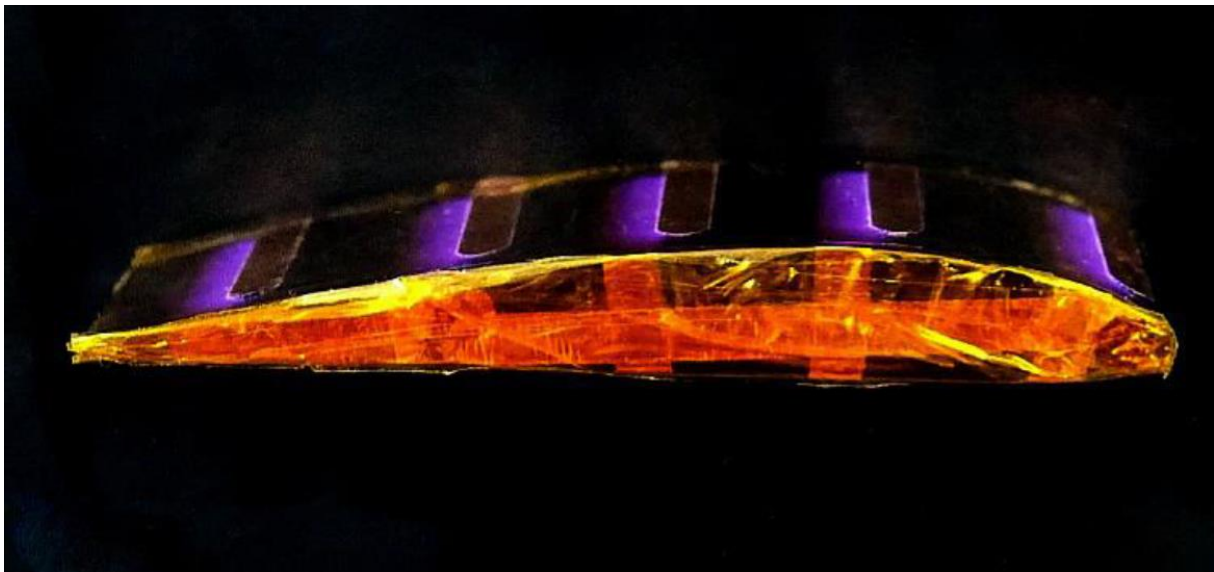


Figure 3: The plasma formation on the airfoil for the 8th configuration

RESULTS

Plasma Actuators on the Flat Plate

The results of the plasma actuators on the flat plate experiments were given in Table 1 and the examples for the experiment images were given in Figure 4. For experiments No. 1-9, the power measurements were taken after plasma formation. Nevertheless, for experiments No. 10-18, after the application of power, the dielectric layers of each of the plasma actuators were burnt. For the dielectric layers with increased thickness and electrode lengths, stable plasma formation was observed (for experiments No. 13-18.), and their working time was long enough for power measurements.

Table 1: Tested plasma actuator parameters and power measurement results

No	Electrode Length (cm)	Dielectric Layer Thickness (mm)	Information About Used Power Supply			Power (W)
			Power Supply Type	Voltage (kV)	Frequency (kHz)	
1	1	0.18	Ozone Generator	15	3	2.6
2	1	0.36				2.4
3	1	0.72				2.3
4	3	0.18				2.8
5	3	0.36				2.5
6	3	0.72				2.4
7	10	0.18				2.9
8	10	0.36				2.6
9	10	0.72				2.5
10	1	0.18	Neon	10	31	NA
11	1	0.36				8.7
12	1	0.72				45
13	3	0.18				90.1
14	3	0.36				53.2
15	3	0.72				76
16	10	0.18				95.8
17	10	0.36				
18	10	0.72				

Setup of the power meter hasn't been made from the high voltage side of the ozone generator power supply, therefore the specified power values are not equal to the power directly consumed by the actuator and this fact should not be neglected. This situation is derived from the energy consumption and the losses during the current is processed in the power supplies.

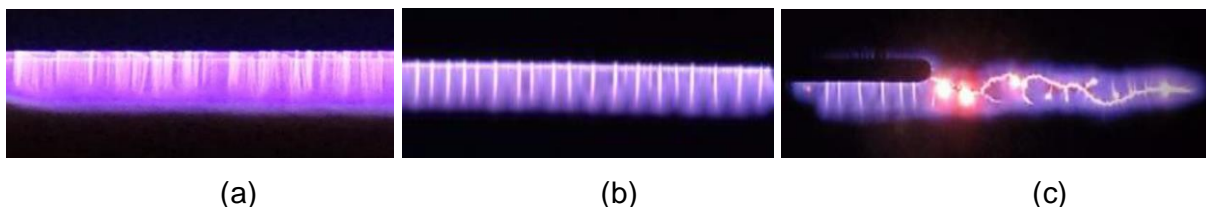


Figure 4: Example results for (a) ozone generator power supply activation (b) neon power supply activation (c) an actuator is being unused with the activation of nonoptimal parameters

It can be seen from Figure 4 that when a plasma actuator was powered by ozone generator, which is operated with 15kV and 3kHz, plasma formation is uniform, streamers are not formed and plasma stays in glow state. However, when neon power supply was used (10kV, 31kHz) plasma tends to localize and forms streamers. For the supplies which have high frequency values, streamers are generated and this causes to reduce thrust-to-power ratio. A power supply that has lower output frequency can be selected for preventing this situation. Furthermore, increasing dielectric layer thickness can be used. However, increasing the

dielectric layer thickness prevents generating an electrical wind as expected velocity. The actuators were burnt after the activation of supplies for the thin dielectric layer thickness. It has been observed that, for the various conditions, using 15kV and 3kHz ozone generator power supply instead of neon power supply is more suitable for plasma activation. The optimum condition can only be handled by this supply.

For the ozone generator power supply, it has been observed that the power consumption increases as the dielectric layer thickness increases for equal electrode length. Because as the dielectric layers thickness decreases, electrons move more easily and the current used by the plasma actuator increases. In the number of equal dielectric layers, it was observed that as the electrode length increases, the energy per unit length decreases. Because the energy per unit length decreased in the plasma generated by the longer electrodes.

For the neon power supply, it has been observed that the power consumption increases as the dielectric layer thickness increases or as the electrode length increases. Because as the number of dielectric layers increases or electrode length increases, the area where plasma forms get larger and the dielectric layers burn.

In order to create a uniform plasma during the wing span, it is thought that 3 cm long electrodes would be suitable in the smoke experiments (for spanwise configurations which can fit the test room). In addition, it is decided to use ozone generator power supply and 0.36 mm dielectric layer thickness. Because the generated electric wind could not be achieved at the desired level when the dielectric layer thickness is more than this value. When the dielectric layer thickness is less than this value, it has been observed that the discharge between two electrodes is high in the less resistant parts of the actuator.

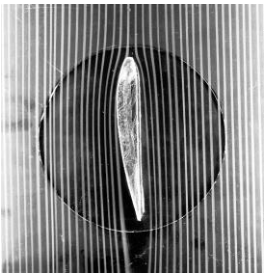
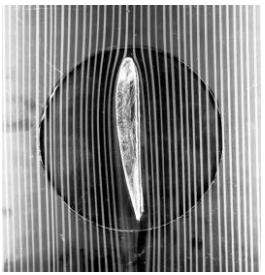
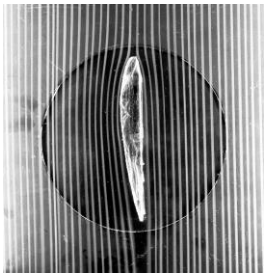
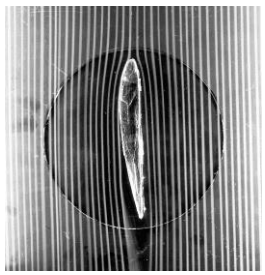
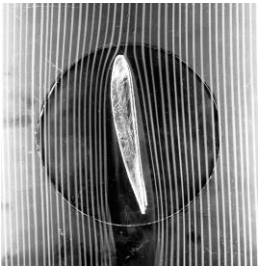
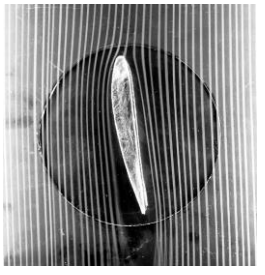
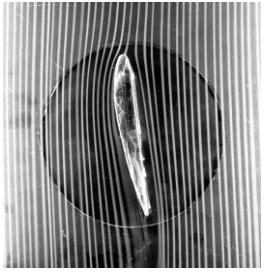
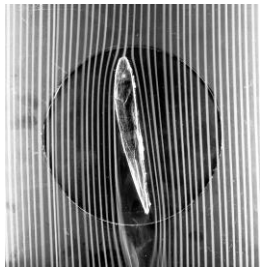
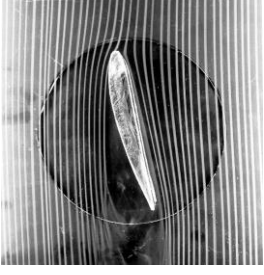
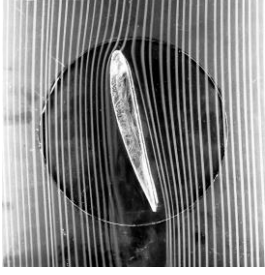
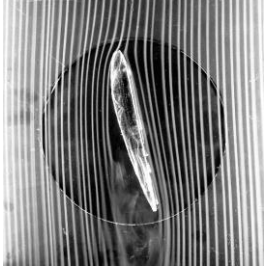
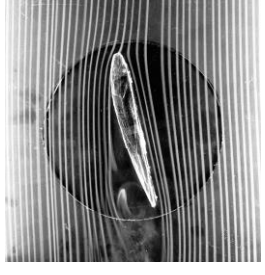
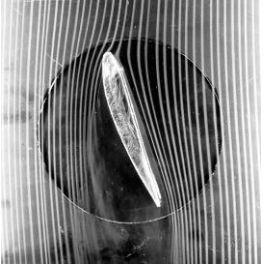

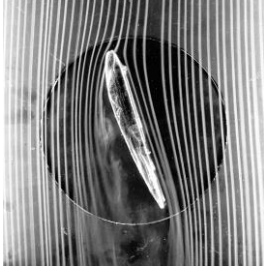

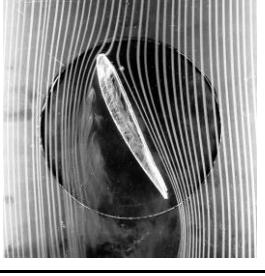



As a result, it has been observed that the plasma actuator which is the most stable, able to generate uniform plasma through the actuator, and able to induct flow in stagnant air that possess 3 cm electrode length, 0.36 mm dielectric layer thickness and using ozone generator power supply for plasma activation were approved. Plasma actuators with these parameters applied on the wing used for smoke tests.

Flow Visualization

Flow visualization results for eight different actuator configurations were given in this part.

Single Actuator Configurations: The results for the plasma actuator configuration No. 1-3 were given in Figure 5. For single actuator configurations, it has been observed that the average power consumption is 2.2 Watt.

In tests in which the plasma actuator is placed as the first configuration, it has been observed that the flow at the wing and especially at the front section of the airfoil can be controlled up to approximately $\alpha=15^\circ$, and after this angle, despite the fact that the control effect is reduced for the airflow in this section, it can still has an effect on the streakline, which comes under the wing, at higher angles. For the second configuration, it has been observed that the plasma actuator creates an effect that converges the streakline to the wing above the point where the electrodes are located. It has been observed that this configuration has a flow control effect up to $\alpha=10^\circ$. At $\alpha=15^\circ$, the effect can be seen slightly, and it disappears after this angle. For the third configuration, it has been observed that the streakline approaches wing from the point near to the rear side of the airfoil. This configuration is efficient from $\alpha=0^\circ$ to $\alpha=5^\circ$ angles of attack. At $\alpha=10^\circ$, the effect can be seen slightly, and it disappears after this angle.

Angle of Attack (deg)	Plasma Off	Plasma On		
		1 st Configuration	2 nd Configuration	3 rd Configuration
0				
5				
10				
15				
20				

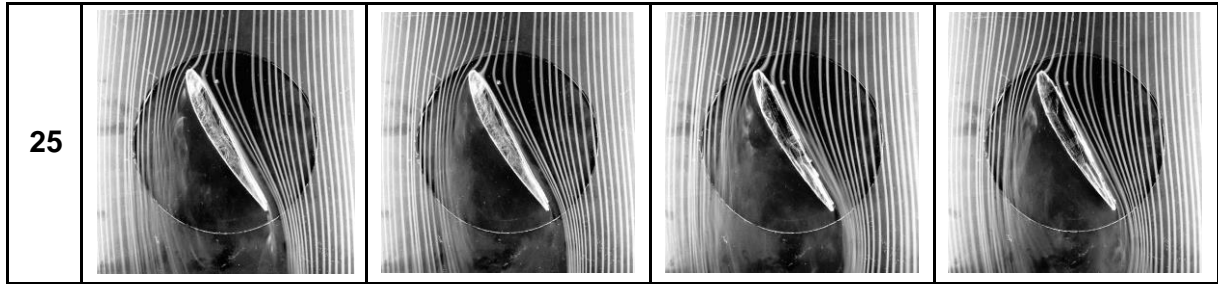
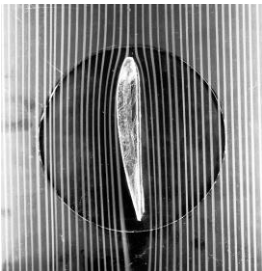
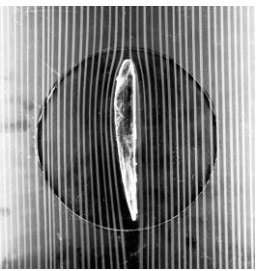
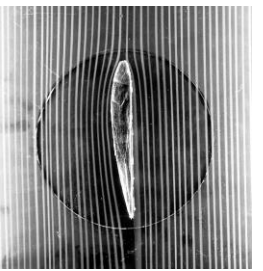
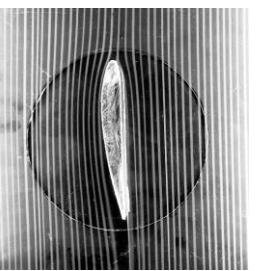
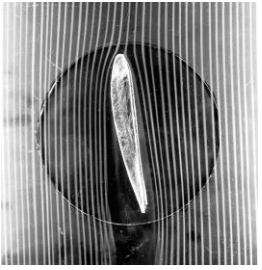
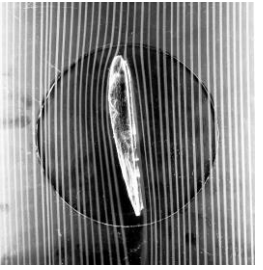
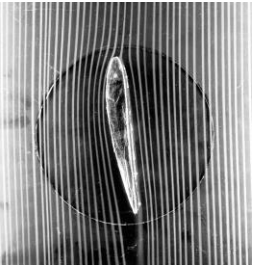
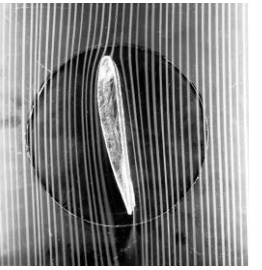


Figure 5: Results for the single plasma actuator configurations

Dual Actuator Configurations: The results for the plasma actuator configuration No. 4-6 were given in Figure 6. For dual actuator configurations, it has been observed that the average power consumption is 2.3 Watt.

In the configurations where the electrodes of the plasma actuator are located as the fourth configuration, it has been observed that there is a flow control effect up to $\alpha=15^\circ$ and after this angle, the effect of plasma can be seen slightly up to $\alpha=25^\circ$. For the fifth configuration, it has been observed that there is a flow control effect up to $\alpha=10^\circ$ and after this angle, the effect of plasma can be seen slightly up to $\alpha=20^\circ$. For the sixth configuration, the effect of plasma actuator can be seen up to $\alpha=10^\circ$ and after this angle, the effect of plasma can be seen slightly up to $\alpha=15^\circ$.

Angle of Attack (deg)	Plasma Off	Plasma On		
		4th Configuration	5th Configuration	6th Configuration
0				
5				

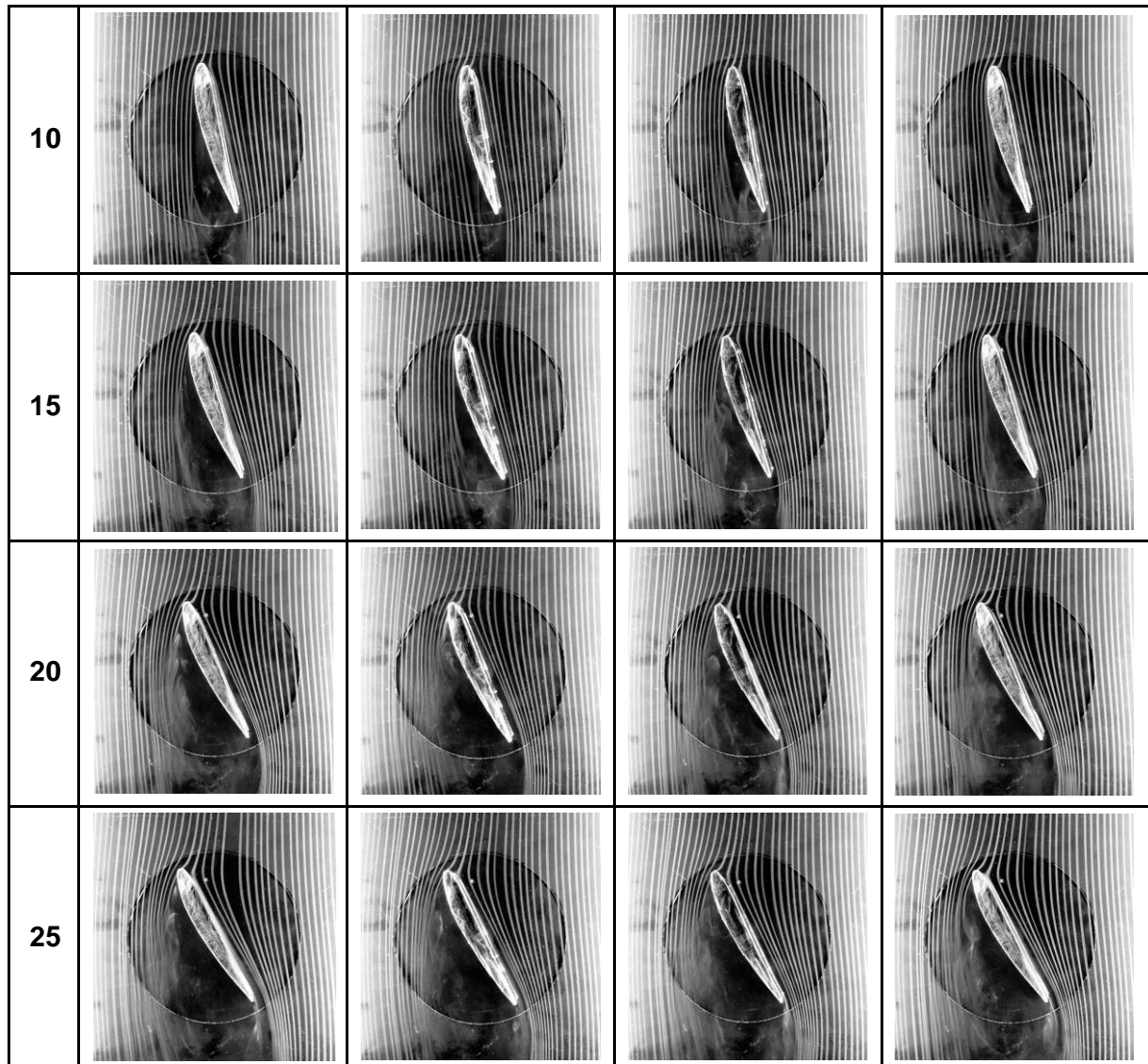
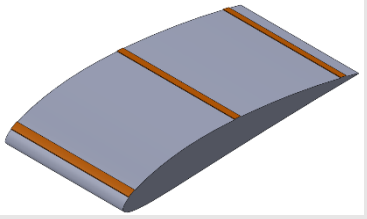
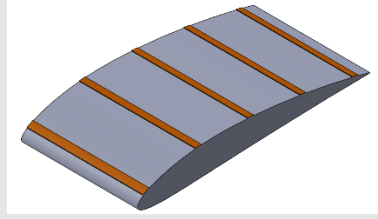
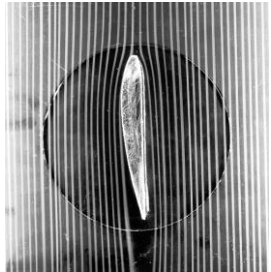
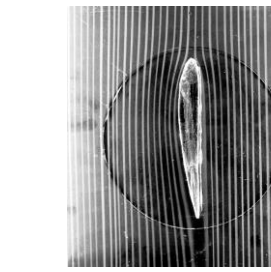
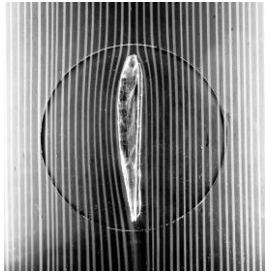
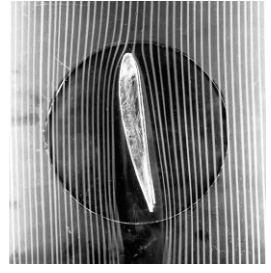
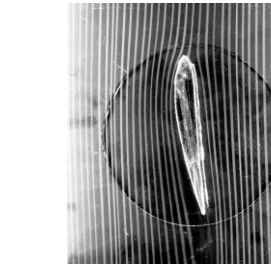
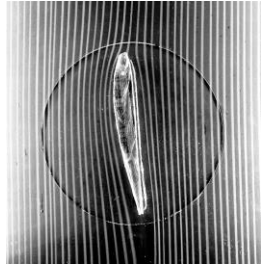
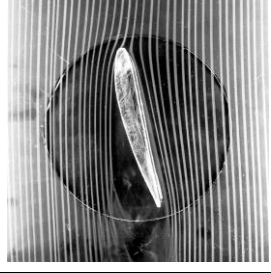
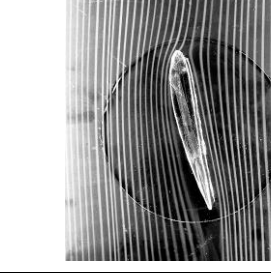
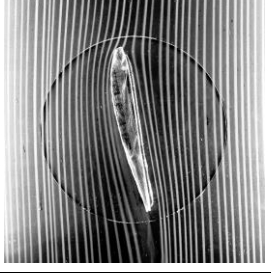
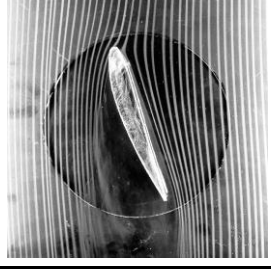
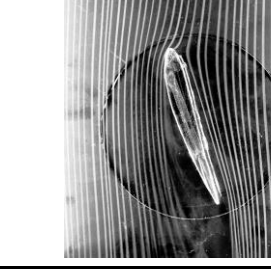
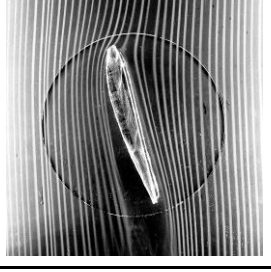
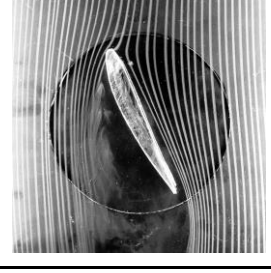
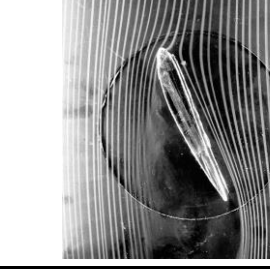
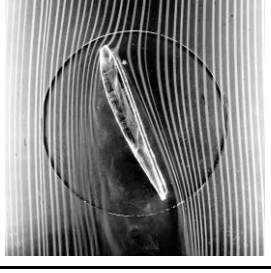


Figure 6: Results for the dual plasma actuator configurations

Seventh and Eighth Actuator Configurations: The results for the plasma actuator configuration No. 7-8 were given in Figure 7. Average power consumption values were observed as 2.4-2.5 Watt for 7th actuator configuration, and 2.6 Watt for 8th configuration.

For the 7th configuration, the effect of the plasma actuator can be seen up to $\alpha=15^\circ$ and can be seen slightly at $\alpha=20^\circ$. For the 8th configuration, the effect of the plasma actuator can be seen up to $\alpha=15^\circ$ obviously. The effect can be seen slightly up to $\alpha=25^\circ$. The widest operating range has been observed at the eighth actuator configuration as it combines the effects of all other configurations. A very effective flow control has been reached until $\alpha=20^\circ$, and it continued to carry on its effectiveness slightly at $\alpha=25^\circ$.

Angle of Attack (deg)	Plasma Off	Plasma On	
		7 th Configuration	8 th Configuration
			
0			
5			
10			
15			
20			

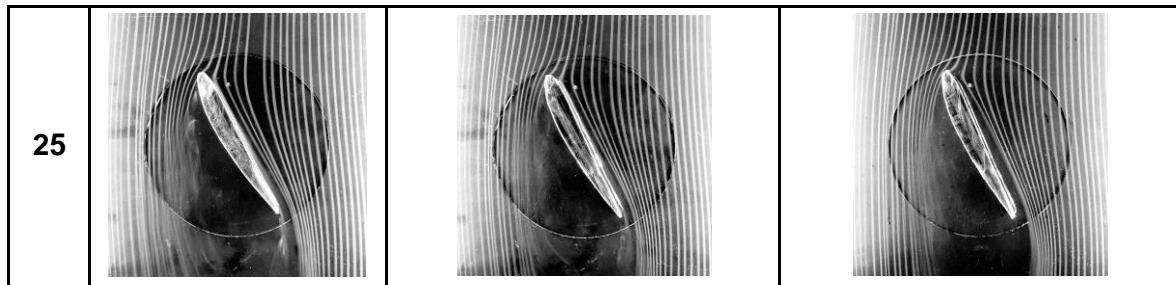


Figure 7: Results for the 7th and 8th plasma actuator configurations

As a result; when the actuators are located near the leading edge of the airfoil, flow control is the most effective at high angles of attack. On the contrary, flow control of the half chord located actuator is the most efficacious at moderate angles of attack, and the actuators that are located near the rear side of the airfoil have high effect at low angles of attack. By using multiple electrodes on various locations of the airfoil, flow control is better as the single actuators' effect on approaching the streakline to the airfoil surface is combined. In addition, as each singly powered electrode configuration (i.e. A, C and E) is effective at different angles of attack, for multiple electrode configurations (e.g. A+C+E), their effectiveness is combined and a wider operating range is obtained for the airfoil. This point is important because the total power was nearly the same for the single and multiple electrode configurations, that is power per unit area decreases as the number of actuators increases. Images similar to the streakline images taken at the plasma off state of the NACA 4412 airfoil when it's at leading edge stall at $\alpha=14^\circ$ angle of attack can be seen at higher angles of attack when the plasma is on (Abbot et al., 1945). It's been estimated that the plasma actuator delays the stall angle with its flow control effect, however a clear interpretation cannot be done with these experiments.

CONCLUSION

From the flat plate tests, it has been observed that the plasma actuator which is the most stable, able to generate uniform plasma through the actuator, and able to induct flow in stagnant air possess 3 cm electrode length, 0.36 mm dielectric layer thickness and using ozone generator power supply instead of neon power supply is more suitable for activation. Plasma actuators with these parameters applied on the wing used for smoke visualization tests.

From flow visualization tests it has been observed that each actuator configuration has an effect on flow control. Each configuration has high effect at different angles of attack. The actuator on the front side of the airfoil has higher effect at high angles of attack, the actuator on half chord has higher effect at moderate angles of attack, and the actuator on the rear side of the airfoil has higher effect at low angles of attack. For this reason, the flow control is better for the actuator configurations in which has multiple electrodes were powered along the chord line, as the single actuators' effect is combined and the stall is delayed.

As future works, wind tunnel testing with a larger wing with the same plasma actuator configurations will be carried out with the help of the results of smoke visualization tests. In wind tunnel experiments, lift and drag force coefficients of the wing will be calculated and the effects of the plasma actuator on the aerodynamic performance will be evaluated.

ACKNOWLEDGEMENTS

This study is carried out with the support of the Scientific and Technological Research Council of Turkey (TÜBİTAK), as part of the 2209-A Research Project Support Programme for Undergraduate Students (project number: 1919B012000994)

References

- Abbot, I. H., Von Doenhoff, A. E., and Stivers, L. S. (1945). *Summary of Airfoil Data*. NACA Repor No 824 (p. 265).
- Akansu, Y. E., Karakaya, F., and Şanlısoy, A. (2013). Active control of flow around NACA 0015 airfoil by using DBD plasma actuator. *EPJ Web of Conferences*, 45. <https://doi.org/10.1051/epjconf/20134501008>
- Al-Sadawi, L., Chong, T. P., and Kim, J. H. (2019). Aerodynamic noise reduction by plasma actuators for a flat plate with blunt trailing edge. *Journal of Sound and Vibration*. <https://doi.org/10.1016/j.jsv.2018.08.029>
- Cattafesta, L. N., and Sheplak, M. (2011). Actuators for Active Flow Control. *Annual Review of Fluid Mechanics*, 43(1), 247–272. <https://doi.org/10.1146/annurev-fluid-122109-160634>
- Greenblatt, D., Göksel, B., Rechenberg, I., Schüle, C. Y., Romann, D., and Paschereit, C. O. (2008). Dielectric barrier discharge flow control at very low flight Reynolds numbers. *AIAA Journal*, 46(6), 1528–1541. <https://doi.org/10.2514/1.33388>
- Jurnal, G., Kose, C., Kolbakir, C., Durna, A. S., and Karadag, B. (2021). Improvement of smoke rakes and the image processing for the flow visualization experiments. *11th Ankara International Aerospace Conference, September 2021 (Accepted)*.
- Karadag, B., Cho, S., Funaki, I., Hamada, Y., and Komurasaki, K. (2018). External Discharge Plasma Thruster. *J. Propuls. Power*, 34(4), 1094–1096.
- Karadag, B., Kolbakir, C., & Durna, A. S. Plasma Actuation Effect on a NACA 4412 Airfoil. (2021). *Aircraft engineering and aerospace technology*, Vol. ahead-of-print, No. ahead-of-print. <https://doi.org/10.1108/AEAT-04-2021-0101>.
- Kolbakir, C., Liu, Y., Hu, H., and Hu, H. (2019). An Experimental Study on the Effects of the Layout of DBD Plasma Actuators on Its Anti-/De-Icing Performance for Aircraft Icing Mitigation. *SAE Technical Papers, 2019-June*, 1–7. <https://doi.org/10.4271/2019-01-2033>
- Little, J., Nishihara, M., Adamovich, I., and Samimy, M. (2010). High-lift airfoil trailing edge separation control using a single dielectric barrier discharge plasma actuator. *Experiments in Fluids*. <https://doi.org/10.1007/s00348-009-0755-x>
- Moreau, E. (2007). Airflow control by non-thermal plasma actuators. *Journal of Physics D: Applied Physics*, 40(3), 605–636. <https://doi.org/10.1088/0022-3727/40/3/S01>
- Neretti, G. (2016). Active Flow Control by Using Plasma Actuators. In *Recent Progress in Some Aircraft Technologies*. InTech. <https://doi.org/10.5772/62720>
- Post, M. L., & Corke, T. C. (2004). Separation control on high angle of attack airfoil using plasma actuators. *AIAA Journal*. <https://doi.org/10.2514/1.2929>
- Starikovskaia, S. M. (2006). Plasma assisted ignition and combustion. In *Journal of Physics D: Applied Physics*. <https://doi.org/10.1088/0022-3727/39/16/R01>
- Thomas, F. O., Corke, T. C., Iqbal, M., Kozlov, A., and Schatzman, D. (2009). Optimization of dielectric barrier discharge plasma actuators for active aerodynamic flow control. *AIAA Journal*. <https://doi.org/10.2514/1.41588>